Significance of Glycine 478 in the Metabolism of *N*-Benzyl-1-aminobenzotriazole to Reactive Intermediates by Cytochrome P450 2B1[†]

Ute M. Kent,[‡] Imad H. Hanna,[‡] Grazyna D. Szklarz,[§] Alfin D. N. Vaz,[∥] James R. Halpert,[§] John R. Bend,[⊥] and Paul F. Hollenberg*,[‡]

Departments of Pharmacology and Biochemistry, The University of Michigan, Ann Arbor, Michigan 48109, Department of Pharmacology and Toxicology, University of Arizona, Tucson, Arizona 85721, and Department of Pharmacology and Toxicology, University of Western Ontario, London, Canada N6A 5C1

Received May 7, 1997; Revised Manuscript Received July 7, 1997[⊗]

ABSTRACT: The effect of mutating Gly 478 to Ala in rat cytochrome P450 2B1 on the metabolism of *N*-benzyl-1-aminobenzotriazole was investigated. The 7-ethoxy-4-(trifluoromethyl)coumarin *O*-deethylation activity of the wild-type enzyme was completely inactivated by incubating with 1 μM BBT. The G_{478}A mutant, however, was not inactivated by incubating with up to 10 μM BBT. Whereas metabolism of BBT by the wild-type 2B1 resulted in the formation of benzaldehyde, benzotriazole, aminobenzotriazole, and a new metabolite, the G_{478}A mutant generated only the later. This metabolite was found by NMR, IR, and mass spectrometry to be a dimeric product formed from the reaction of two BBT molecules. Two spectral binding constants, a high-affinity constant that was the same for both enzymes (30−39 μM) and a low-affinity constant that was 5-fold lower for the mutant enzyme (0.3 mM vs 1.4 mM), were observed with BBT. The apparent K_m and k_{cat} values for the G_{478}A mutant with BBT were 0.3 mM and 12 nmol (nmol of P450)$^{-1}$ min^{-1}, respectively. Molecular modeling studies of BBT bound in the active site of P450 2B1 suggested that a mutation of Gly 478 to Ala would result in steric hindrance and suppress oxidation of BBT at the 1-amino nitrogen. When BBT was oriented in the 2B1 active site such that oxidation at the 7-benzyl carbon could occur, no steric overlap between Ala 478 and the substrate was observed. Thus, this orientation of BBT would be preferred by the mutant leading to oxidation at the 7-benzyl carbon and subsequent dimer formation. These findings indicate that a glycine 478 to alanine substitution in P450 2B1 altered the binding of BBT such that inactivating BBT metabolites were no longer generated.

The endoplasmic reticulum cytochrome P450[1] system is composed of multiple P450 monooxygenases and NADPH−P450 reductase. This enzyme system is responsible for the oxidative metabolism of exogenous (drugs, pesticides, environmental pollutants, carcinogens) and endogenous (steroids, prostaglandins, retinoids, alkaloids, lipophilic vitamins) compounds (*2*). Although the numerous forms of P450 enzymes often display overlapping substrate specificities, individual isoforms may be very selective for certain compounds (*3*−*6*). The important role these enzymes play in the detoxification or activation of xenobiotics to potentially carcinogenic or toxic compounds has generated a strong interest in identifying the critical amino acid residues involved in substrate binding and catalysis (*4*). Currently, only the three-dimensional structures of soluble bacterial cytochromes are available. Therefore, functionally important amino acid residues of mammalian cytochromes have been identified by site-directed mutagenesis, photoaffinity labeling, mechanism-based inactivation, and amino acid sequencing of the modified peptides and by comparing naturally occurring mutations in a number of different allelic variants (*6*−*16*).

Cytochrome P450 2B1 is the major phenobarbital-inducible P450 enzyme in rat liver. In the rat 2B subfamily several allelic variants have been demonstrated by two-dimensional electrophoresis or protein and DNA sequencing (*17*). When compared with 2B1 from outbred Sprague-Dawley rats, the purified P450 2B1 from Wistar−Munich rats exhibited 5-fold lower androstenedione 16β-hydroxylation, testosterone 16-hydroxylation, and 7-ethoxycoumarin *O*-deethylation activities but elevated levels of androstenedione 16α-hydroxylation activity (*6*). Kedzie *et al.* showed that the androstenedione 16β-hydroxylation activity of either microsomes or purified P450 2B1 from phenobarbital-induced inbred Wistar−Munich rats was insensitive to inactivation by the chloramphenicol analog *N*-(2-*p*-nitrophenethyl)chlorofluoroacetamide (*6*). The 2B1 cDNA from Wistar−Munich rats was sequenced, and a single amino acid change at glycine 478 to alanine was found, suggesting that this residue may be

[†] Supported in part by NIH Grant CA 16954 (P.F.H.), NIH Grant ES 03619 and Core Center Grant P30 ES 06694 (J.R.H.), and Medical Research Council of Canada Grant MT-9972 (J.R.B.).

* To whom correspondence should be addressed at the Department of Pharmacology, Medical Science Research Building III, 1150 West Medical Center Drive, Ann Arbor, MI 48109-0632. E-mail: phollen@umich.edu. Fax: 313-763-4450.

[‡] Department of Pharmacology, The University of Michigan.

[§] University of Arizona.

[∥] Department of Biochemistry, The University of Michigan.

[⊥] University of Western Ontario.

[⊗] Abstract published in *Advance ACS Abstracts,* September 15, 1997.

[1] Abbreviations: P450, cytochrome P450; P450 2B1 [nomenclature from Nelson et al. (*1*)], major phenobarbital-inducible P450 in rats; P450 r2B1, N-terminally modified rat P450 2B1 expressed in *Escherichia coli*; P450 r2B1 G_{478}A, N-terminally modified rat P450 2B1 with an alanine to glycine substitution at position 478; P450 101, the cytochrome P450 camphor monooxygenase from *Pseudomonas putida*; reductase, NADPH−cytochrome P450 reductase; ABT, 1-aminobenzotriazole; BBT, *N*-benzyl-1-aminobenzotriazole; DLPC, L-α-dilauroylphosphatidylcholine; PCR, polymerase chain reaction; 7-EFC, 7-ethoxy-4-(trifluoromethyl)coumarin.

S0006-2960(97)01064-7 CCC: $14.00

involved in substrate binding and orientation (*6*). When glycine 478 was replaced with eight amino acids of different size, charge, or hydrophobicity, it was observed that the alanine mutant had a 10-fold lower androstenedione 16β:16α hydroxylase ratio as compared with the wild-type enzyme (*10*).

A three-dimensional model for cytochrome P450 2B1 has been proposed on the basis of the crystal structure of P450 101 (*18*). This model was consistent with the site-directed mutagenesis data. In the model, replacement of glycine 478 with alanine resulted in van der Waals overlaps with androstenedione such that the substrate could not be bound in the 16β orientation.

Benzyl-1-aminobenzotriazole has been shown to be a selective mechanism-based inactivator of P450 2B isoforms and to bind covalently to microsomes from liver or lung guinea pigs (*19*−*21*). Previous studies with purified reconstituted P450 2B1 demonstrated that BBT was metabolized to 1-aminobenzotriazole, benzotriazole, benzaldehyde, and a novel unidentified product, #27, and that the mechanism-based inactivation of BBT was primarily due to binding of a BBT metabolite to the P450 protein (*22*).

The current study shows that a single glycine to alanine change at position 478 in P450 2B1 abolished the formation of the inactivating species of BBT. These data were interpreted with the help of molecular modeling. A novel finding of this work was that the oxidation of BBT resulted in the formation of a dimer by both the wild-type and the mutant enzyme. In combination with spectral data, these observations suggested that two molecules of BBT may be accommodated by P450 2B1. The present study further illustrates the feasibility of the P450 2B1 active site model in the design of specific mechanism-based inactivators to selectively target very closely related P450 isoforms.

EXPERIMENTAL PROCEDURES

Materials. Bacto tryptone and Bacto yeast extract were from DIFCO (Detroit, MI). T4 ligase, pALTER 1 vector, JM 109 cells, and restriction enzymes were obtained from Promega (Madison, WI). L-α-Dilauroylphosphatidylcholine, NADPH, benzphetamine, *n*-octylamine, δ-aminolevulinic acid, resorufin, and catalase were purchased from Sigma Chemical Co. (St. Louis, MO). 7-Pentoxyresorufin, benzyloxyresorufin, and 7-ethoxy-4-(trifluoromethyl)coumarin were obtained from Molecular Probes Inc. (Eugene, OR), and 7-hydroxy-4-(trifluoromethyl)coumarin was from Enzyme Systems Products (Livermore, CA). *N*-Benzyl-1-aminobenzotriazole and 1-aminobenzotriazole were gifts from Dr. J. M. Mathews (Research Triangle Institute, Research Triangle Park, NC). [^{14}C]-7-BBT with a specific activity of 3.23 mCi/mmol was synthesized as previously described (*23*). MV1304 cells were a gift from Dr. S. Pernecky (Eastern Michigan University, Ypsilanti, MI). Primers for polymerase chain reaction and site-directed mutagenesis were obtained from the University of Michigan Macromolecular Core Facility (Ann Arbor, MI.) pCW Ori$^+$, a derivative of the PHSe5 plasmid, was kindly provided by Dr. F. W. Dahlquist (University of Oregon, Eugene, OR).

Site-Directed Mutagenesis. A mutation at glycine 478 to alanine in rat P450 2B1 that had a slight N-terminal modification to facilitate expression in *Escherichia coli* was introduced by PCR essentially as previously described (*24*). pCW Ori$^+$ 2B1 plasmid (10 μg) was digested with *Kpn*I and *Eco*RI in Multicore buffer (Promega, Madison, WI) for 1 h at 37 °C. The resulting 400 bp fragment was resolved on a 1% agarose gel, excised, and purified using an 0.45 μM Ultrafree-MC centrifugal filter device as described by the manufacturer (Millipore, Bedford, MA). The purified fragment was ligated into pALTER 1. Competent JM 109 cells were transformed and selected by plating on Luria−Bertani plates containing 10 μg of tetracycline/mL (*26*). Individual tetracycline-resistant colonies were picked and used to inoculate 3 mL of Luria−Bertani media containing 10 μg of tetracycline/mL. The 3 mL cultures were grown overnight at 37 °C with vigerous shaking (300 rpm). Plasmid DNA from the bacterial cultures was isolated using the Wizard Minipreps DNA isolation kit (Promega, Madison, WI) according to the manufacturer's protocol. The incorporation of the 2B1 *Kpn*I/*Eco*RI fragment into the multicloning site of the pALTER plasmid (to generate cloneKE) was confirmed by diagnostic restriction enzyme analysis. Substitution of P450 2B1 glycine 478 with alanine was performed by two consecutive rounds of PCR using the cloneKE plasmid. The first round of PCR was performed in two separate tubes. Each reaction mixture contained 1 × *pfu* reaction buffer, 1.0 mM dNTPs, 5 fmol of cloneKE plasmid, and 1.25 units of recombinant *pfu* polymerase (Stratagene, La Jolla, CA). To the first tube was added 100 pmol of the sense primer (5′-GAGGTATTTTTGCAATGCCACT-3′) spanning the sequence corresponding to Gly 478 together with 100 pmol of T7 (5′-AGTGGCATTGCAAAAATACCTC-3′) promoter primer. The second reaction contained 100 pmol of antisense primer (5′-AGTGGCATTGCAAAAATAC-CTC-3′) together with 100 pmol of SP6 promoter primer (5′-GACCATGATTACGCCAAGC-3′). The overlapping products of the two reactions (94 and 376 bp) were purified using Centricon concentrators with a 50 000 MW cutoff (Amicon, Beverly, MA). For the second round of PCR 15 fmol of each product was combined and subjected to 10 rounds of PCR to ensure adequate 3′ extension of the heteroduplex templates. The outside primers (T7 and SP6, 100 pmol of each in 1 μL) were added, and 30 more PCR cycles were performed. The resulting 470 bp PCR product was purified with UltrafreeMC filters (100 000 MW cutoff, Millipore, Bedford, MA), digested with *Kpn*I and *Eco*RI, and used to replace the corresponding fragment in pCW2B1. The incorporation of the G478A mutation was confirmed by sequencing the pCW2B1 G478A plasmid using the RG2 (5′-AGAGCTGGGGCACCT-3′) located at position 1492 relative to the 2B1 cDNA start codon and T7 as primers.

Expression of Proteins. E. coli MV 1304 cells containing either pCW2B1 (coding for rat P450 r2B1) or pCW2B1-G_{478}A (coding for rat P450 r2B1 G_{478}A) were grown in 50 mL of modified terrific broth containing 12 g of bactopeptone/L, 24 g of yeast extract/L, 4 mL of glycerol/L, 55 mM dibasic potassium phosphate, 17 mM monobasic potassium phosphate, pH 7.2, 1 mM thiamin, 0.5 mM ammonium ferrous sulfate, and 100 μg of ampicillin/mL at 300 rpm for 3 h at 37 °C. Cells were expanded to 1 L of modified terrific broth in 2.8 L Fernbach flasks and grown for 1 h at 37 °C while being shaken. Then 0.5 mM δ-aminolevulenic acid was added, and cells were grown at 225 rpm while the temperature was gradually dropped to 27 °C. Once the temperature had reached 27 °C (approximately 1−1.5 h), 1.5 mM IPTG was added to induce P450 expression and

the culture was maintained at 27 °C for 15−20 h in a shaking incubator at 180 rpm.

Rat NADPH−P450 reductase was expressed in *E. coli* Topp3 cells (Stratagene, La Jolla, CA) transformed with the rat reductase containing the expression plasmid pOR263 (*27*) as described.[2]

Purification of Proteins. Cells were harvested, and the P450s were purified essentially as described by Guengerich (*25*) with minor modifications.[2] P450 r2B1 and P450 r2B1 $G_{478}A$ were purified from solubilized bacterial membranes by chromatography on DEAE-Sephacel followed by hydroxyapatite chromatography. The specific content of r2B1 was 6.6 nmol of P450/mg of protein and that of r2B1 G478A was 7.4 nmol of P450/mg of protein.

Rat NADPH−P450 reductase was purified from bacteria as described[2] with minor modifications. Bacterial membranes were solubilized at 5 mg/mL in 100 mM Tris-HCl (pH 7.7), 20% glycerol, 1 mM EDTA, 1 mM DDT, 10 mM CHAPS, 1 μM FMN, 10 μg of aprotinin/mL, 2 μM leupeptin, 0.1 mM PMSF, and 0.1% Tergitol at 4 °C overnight in the dark. The purity of reductase was approximately 9 nmol of reductase/mg of protein as estimated from the flavin spectrum.

Microsomal Membranes. Microsomal membranes were prepared from the livers of fasted male Fischer or Wistar−Munich rats (175−190 g, Harlan Sprague-Dawley, Indianapolis, IN) given 0.1% phenobarbital in their drinking water for 12 days (*28*).

Enzyme Activity Assays. The effect of BBT on the 7-pentoxyresorufin *O*-deethylation activity was tested in microsomes from Fischer or from Wistar−Munich rats. Microsomes were suspended at 1.2 nmol/mL in 50 mM Tris-HCl (pH 7.5), 5 mM $MgCl_2$, and BBT (in 10 μL of DMSO/mL) or 10 μL of DMSO/mL. The reaction was equilibrated for 3 min at 30 °C before addition of 1.2 mM NADPH (primary reaction). At 0, 0.5, 3.5, 6.5, and 9.5 min, 20 μL aliquots of the primary reaction mixture were transferred into a secondary reaction mixture containing 5 μM 7-pentoxyresorufin, 5 mM $MgCl_2$, and 0.2 mM NADPH in 50 mM Tris-HCl (pH 7.5). Fluorescence was monitored for 99 s on a SLM-Aminco Model SPF-500 C spectrofluorometer with an excitation at 522 nm and emission at 586 nm (*29*). Enzymatic activity was determined by comparing the fluorescence change to a standard curve generated from resorufin.

The activity of the purified, reconstituted P450 enzymes was measured using 7-ethoxy-4-(trifluoromethyl)coumarin as a substrate. The remaining 7-EFC *O*-deethylation activity of samples incubated with 0, 1, 5, or 10 μM BBT or 1 mM ABT was measured spectrophotometrically as described previously (*22, 30*).

The formation of formaldehyde from benzphetamine was measured as described by Nash (*31*). P450, either 1 μM r2B1 or 1 μM r2B1 $G_{478}A$, was reconstituted with reductase and 200 μg of DLPC/mL at a molar concentration of 1:1, 1:2, or 1:3 or together with cytochrome b_5 at a molar ratio of 1:2:2 of P450:reductase:b_5 for 1 h at 4 °C. The reconstituted enzymes were diluted to 445 μL with 50 mM potassium phosphate (pH 7.4). To each sample was added 50 μL of 4.15 mg of benzphetamine/mL of H_2O, and the samples were equilibrated at 37 °C for 3 min. Reactions were initiated by addition of 5 μL of NADPH to a final concentration of 1 mM. After 20 min at 37 °C, the reactions were quenched with 250 μL of ice-cold 60% trichloroacetic acid. Precipitated protein was pelleted by centrifugation, and 500 μL of the supernatant was mixed with 250 μL of Nash reagent (7.8 M ammonium acetate, 82 mM 2,4-pentanedione). The mixtures were incubated for 35 min at 37 °C. The absorbance at 412 nm was measured spectrophotometrically, and the amount of formaldehyde formed was calculated from a standard curve.

Determination of K_m and k_{cat}. Cytochrome P450 $G_{478}A$ was reconstituted with reductase and DLPC as described for the 7-EFC *O*-deethylation assays. Each duplicate reaction contained 0.1 nmol of P450 $G_{478}A$ in a final volume of 100 μL and 0−2.56 mM BBT (28.8 μCi/mmol BBT) in 2 μL of DMSO. The samples were equilibrated at 30 °C for 3 min, and the reactions were initiated with 1.2 mM NADPH. After 10 min at 30 °C the products were extracted three times with 1 mL of ethyl acetate. The organic phases were pooled, evaporated under N_2, and analyzed by reversed-phase HPLC as previously described (*22*). The quantity of #27 recovered was determined after liquid scintillation counting. Rates were calculated, and the K_m and k_{cat} were obtained from nonlinear regression analysis using the Enzyme Kinetics program version 1.04 from Trinity Software.

Identification of #27. High-resolution proton or ^{13}C NMR spectra were obtained by Scott Woehler in the College of Pharmacy, The University of Michigan, on a Bruker Avance DRX500 spectrophotometer using the XWIN-NMR 1.1.1 program. Proton NMR spectra were acquired at room temperature for 1 h with an inverse detection probe using a standard pulse, a sweep width of 20 ppm, and a 1 s recycling time. Data were processed with 32K total points and an exponential filter generating 0.1 Hz line broadening.

^{13}C NMR spectra were acquired at room temperature with a 5 mm broad-band commercial probe for 36 h using a 90° pulse, a sweep width of 315.5 ppm, and a 3 s recycle time. Data were processed with 64K total points and an exponential filter generating 3 Hz line broadening.

Electrospray mass spectrometry and laser desorption mass spectrometry analyses were performed at the University of Michigan Protein and Carbohydrate Structure Facility. Electrospray ionization mass spectra were obtained using a Vestec electrospray source and model 201 single quadrupole mass spectrometer (Vestec Corp., Houston, TX) fitted with a 2000 *m/z* range. Laser desorption mass spectrometry was performed on a Vestec Lasertec MALDI linear time-of-flight mass spectrometer with the laser set at 327 nm (Perseptive Biosystems, Cambridge, MA).

Fast atom bombardment and FT-IR spectrophotometry were performed with the help of Jim Windak in the instrument facility of the Department of Chemistry, The University of Michigan. A Nicolet 60-FX spectrophotometer with a microbeam accessory was used for the FT-IR spectroscopy.

Radiolabeled #27 was obtained by incubating P450 2B1 $G_{478}A$ with [^{14}C]-7-BBT labeled at the 7 position of the benzyl carbon as previously described (*22*). Samples containing 2 μmol of benzoic acid, benzaldehyde, or benzylhydrazine were spiked with radiolabeled #27. The samples were hydrolyzed with 6 M HCl at 110 °C for 18 h. The acid hydrolysates were analyzed by reverse-phase HPLC on a C_{18} μBondapak column using a linear gradient of 95% H_2O/

[2] I. Hanna, J. F. Teiber, K. Kokones, and P. F. Hollenberg, submitted for publication.

5% CH_3OH for 2 min that was increased to 75% H_2O/25% CH_3OH over the subsequent 5 min and then to 20% H_2O/80% CH_3OH. One-milliliter fractions were collected and analyzed for radioactivity by liquid scintillation counting. The retention time of the radioactive peak was compared with the retention times of acid-hydrolyzed benzoic acid, benzaldehyde, and benzylhydrazine standards.

Metabolite Analysis. Products from BBT metabolism by P450 2B1 and P450 2B1 $G_{478}A$ were isolated and resolved by HPLC as previously described except that the final concentration of CH_3OH was 81% (*22*).

Spectral Determinations. P450, either 1 nmol of r2B1 or 1 nmol of r2B1 $G_{478}A$, was incubated with 100 μg of DLPC for 30 min at 4 °C. The reconstituted proteins were diluted to 0.5 μM with 50 mM potassium phosphate (pH 7.4). The samples were divided and placed in the reference and sample cuvettes and scanned from 350 to 500 nm before and after each addition of substrate on a DW 2 UV/visible spectrophotometer (SLM Aminco, Urbana, IL) equipped with an OLIS spectroscopy operating system (On-Line Instrument Systems, Inc., Bogart, GA). To the sample cuvette were added 1 μL aliquots of BBT (0−580 μM) or *n*-octylamine (0−14 μM) dissolved in DMSO while the reference cuvette received DMSO only. Spectral binding constants were calculated by linear regression after the inverse of the absorbance change versus the inverse of the BBT concentration was plotted.

Reduced CO spectra were recorded from samples incubated with or without 1 mM ABT before and after incubation with NADPH. After incubation for 5 min at 23 °C, 200 μL aliquots of the primary reaction were removed and diluted with 800 μL of ice-cold 50 mM potassium phosphate (pH 7.4) containing 40% glycerol and 0.6% Tergitol NP-10. Spectra were recorded as previously described according to Omura and Sato (*22*, *32*).

Molecular Modeling of Benzphetamine or BBT in the Active Site of 2B1. The molecular model of P450 2B1 was constructed previously (*33*), and the structures of benzphetamine and BBT were constructed using the Builder module of InsightII (Biosym/MSI, San Diego, CA). The 3-D structures were displayed on a Silicon Graphics workstation. Energy minimization and molecular dynamics calculations were carried out with the Discover program (Biosym/MSI, San Diego, CA) using the consistent valence force field (cvff) for simulations with benzphetamine and cvff91 for simulations with BBT.

Benzphetamine was docked into the active site of the P450 2B1 model with its N atom at a distance of 4.7 Å from the heme iron and aligned with the heme Fe and the S of Cys-436 to allow for substrate *N*-demethylation. Conformational analysis of benzphetamine was performed with the Search Compare module of InsightII and was followed by molecular dynamics simulations to achieve the best fit in the active site. For these simulations, the N atom and the C atoms bonded directly to this nitrogen were fixed, while the rest of the benzphetamine molecule, along with the side chains of protein residues within 5 Å from the substrate, was allowed to move (*34*, *35*). Initially, the system was minimized using the steepest descend method and harmonic potential, with a nonbond cutoff of 10 Å, to a maximum gradient of 5 kcal mol^{-1} $Å^{-1}$. For the subsequent molecular dynamics simulations, the leap-frog algorithm was used. The system was equilibrated for 0.1 ps, and the simulations were continued for 1 ps at 300 K using 1 fs time steps. The system was then minimized again using conjugate gradients to a maximum gradient of 1 kcal mol^{-1} $Å^{-1}$, first the substrate molecule only and then the side chains neighboring the substrate (*34*, *35*). The nonbond interaction energy between the substrate and the protein was evaluated with the Docking module of InsightII.

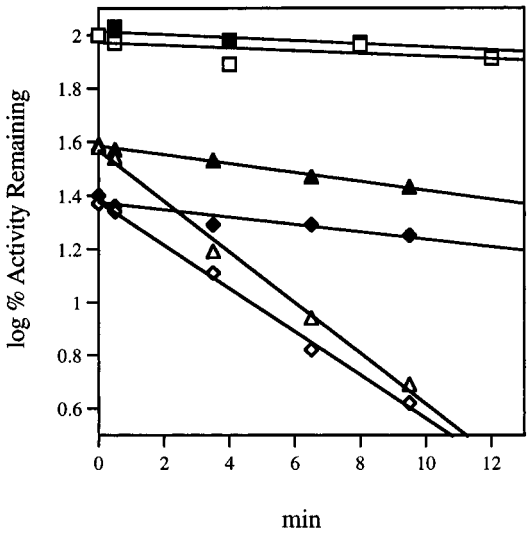

FIGURE 1: Time and concentration-dependent effect of BBT on the 7-pentoxyresorufin *O*-deethylation activity of liver microsomes from phenobarbital-induced Fischer or Wistar−Munich rats. Samples were removed from the primary reaction mixture at the indicated time points and assayed as described under Experimental Procedures. The data shown are representative of two separate experiments each from microsomes of Fischer rats (open symbols) or Wistar−Munich rats (closed symbols). The concentrations of BBT were (□, ■) 0 μM, (△, ▲) 200 μM, and (◇, ◆) 400 μM. The control 100% activity ranged from 3.5 to 3.6 nmol of resorufin formed min^{-1} (nmol of P450)$^{-1}$ for microsomes from Fischer rats and from 1.7 to 2.0 nmol resorufin formed min^{-1} (nmol of P450)$^{-1}$ for microsomes from Wistar−Munich rats.

In the case of BBT, the substrate can be docked at carbon 7 of the benzyl group or at the 1-amino N of the aminobenzotriazole moiety, which would lead to different products. For the initial oxidation event to occur at N, BBT was placed in the active site of P450 2B1 with the N atom at a distance of 4.7 Å from the heme iron, as described for benzphetamine. In the case of oxidation at carbon 7, this atom of BBT was placed at a distance of 5.5 Å from the heme iron to allow for the initial hydrogen abstraction. In both cases, a combination of energy minimization and molecular dynamics was used to refine BBT docking. The oxidation site was kept fixed, and the simulation conditions were as described above for benzphetamine.

RESULTS

Effect of BBT on 2B1 Activity in Microsomes from Fischer or Wistar−Munich Rats. Incubations with BBT in the presence of NADPH resulted in a time- and concentration-dependent decrease in the 7-pentoxyresorufin *O*-deethylation activity in liver microsomes from phenobarbital-treated Fischer rats (Figure 1, open symbols). There was an initial decrease in the activity observed at 0 time that probably reflects competition by the BBT that was carried over into the secondary reaction mixture with 7-pentoxyresorufin. When BBT was incubated with microsomes from Wistar−Munich rats, the same initial drop in activity was seen. However, no significant further loss of activity was observed

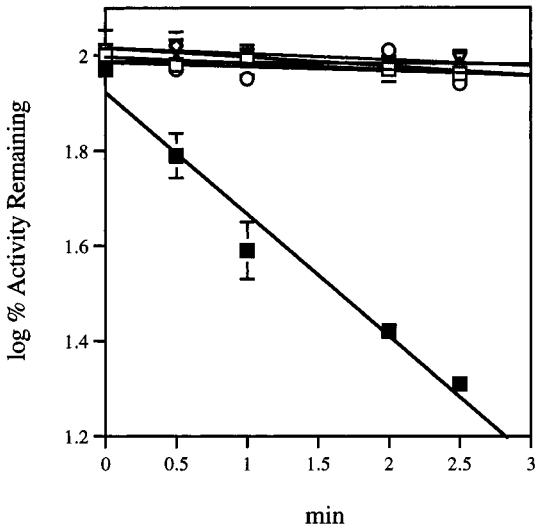

FIGURE 2: Time- and concentration-dependent effect of BBT on the 7-EFC *O*-deethylation activity of expressed P450 r2B1 and P450 $G_{478}A$. Samples were removed from the primary reaction mixture at the indicated time points and assayed for 7-EFC activity as described under Experimental Procedures. Each data point shown represents the mean and standard deviation of three to four experiments. Some errors were smaller than the symbols. For P450 r2B1 the concentrations of BBT were (□) 0 μM and (■) 1 μM. For P450 $G_{478}A$ the concentrations of BBT were (○) 0 μM, (▽) 5 μM, and (◇) 10 μM.

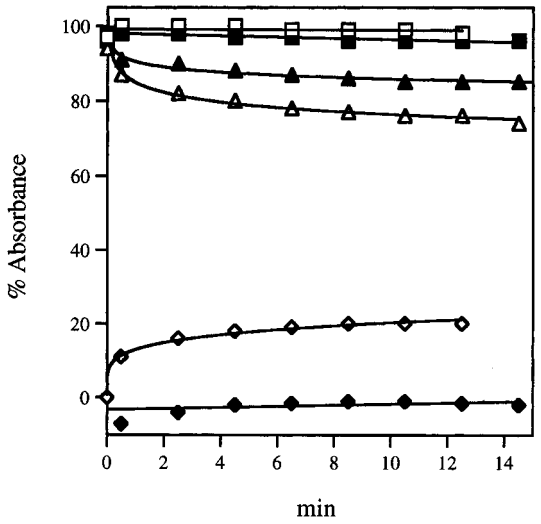

FIGURE 3: Time-dependent spectral changes of expressed P450 r2B1 and P450 $G_{478}A$ during incubation with BBT. Incubations were performed as described in Experimental Procedures. Absorbance of P450 r2B1(open symbols) was at 418 nm when incubated with (□) 0 μM or (△) 10 μM BBT and at 453 nm (◇) when incubated with 10 μM BBT. Absorbance of P450 $G_{478}A$ (filled symbols) was at 418 nm when incubated with (■) 0 μM or (▲) 10 μM BBT and at 453 nm when incubated with (◆) 10 μM BBT. Data shown represent the average of two experiments that did not differ by more than 4%.

over the course of the assay. This result would suggest that unlike the predominant 2B1 form found in Fischer rat microsomes, the allelic variant in Wistar−Munich microsomes was insensitive to inactivation by BBT.

Benzphetamine Oxidation by Reconstituted 2B1. To more clearly characterize the different effects of BBT on the two allelic variants of 2B1, the cDNAs coding r2B1 or r2B1 $G_{478}A$ were expressed in *E. coli* and purified as described under Experimental Procedures. Expression levels were 109 nmol of P450 r2B1/L and 240 nmol of P450 r2B1 $G_{478}A$/L of bacterial culture. The two cytochromes were reconstituted with reductase and DLPC and tested for their ability to oxidize benzphetamine. Both P450 r2B1 and P450 r2B1 $G_{478}A$ were able to generate formaldehyde from benzphetamine at similar rates (23 nmol min^{-1} $nmol^{-1}$ for r2B1 and 21 nmol min^{-1} $nmol^{-1}$ for r2B1 $G_{478}A$). This rate remained the same with increasing molar ratios of P450 to reductase and was unaffected by addition of cytochrome b_5 (data not shown). These results suggest that the mutation of glycine 478 to alanine had not significantly perturbed the structure of the P450 2B1 enzyme and had resulted in a fully active enzyme that was able to generate formaldehyde at the same rate as the wild-type enzyme when incubated under identical conditions.

Effect of BBT on 2B1 Activity in a Reconstituted System. Reconstituted P450 r2B1 or r2B1 $G_{478}A$ was incubated with or without BBT for 0−2.5 min. Figure 2 shows that P450 r2B1 was inactivated by 1 μM BBT in a time-dependent manner. After 2.5 min only 20% residual 7-EFC activity remained compared with incubation mixtures without BBT. When the mutant r2B1 $G_{478}A$ was incubated with 1, 5, or 10 μM BBT, no inactivation was seen compared with control incubations without BBT. Even prolonged incubations for up to 2 h and concentrations as high as 100−200 μM did not result in inactivation of the $G_{478}A$ enzyme and resulted only in a single product, #27 (data not shown).

Effect of BBT on the Heme Spectra of r2B1 and r2B1 $G_{478}A$. After correction for dilution, the absolute spectrum of bacterially expressed r2B1 incubated with 10 μM BBT showed virtually no loss (4−8%) at 418 nm compared with control samples incubated with DMSO. After addition of NADPH, a 22% decrease (compared with 2% for control enzyme incubated without BBT) in the absolute spectrum at 418 nm was seen over the course of 12−14 min (Figure 3, open triangles). Concurrently, a 20% increase in the absorbance at 453 nm was observed (open diamonds). With the mutant $G_{478}A$ enzyme a 15% decrease at 418 nm (filled triangles) was observed compared with 4−5% for the control enzyme incubated without BBT. Virtually no change in the absorbance at 453 nm (filled diamonds) was observed. These spectral observations suggest that BBT interacts with the mutant enzyme differently than with the wild-type enzyme.

Binding Spectra of r2B1 and r2B1 $G_{478}A$. P450 r2B1 or P450 r2B1 $G_{478}A$ was incubated with DLPC, and the binding spectra for *n*-octylamine or BBT were recorded as described in Experimental Procedures. Increasing concentrations of *n*-octylamine produced Type II spectra for both enzymes (data not shown) (*36*, *37*). The binding constants calculated for r2B1 and r2B1 $G_{478}A$ with *n*-octylamine were 1.4 and 1.1 μM, respectively.

Type I spectra were observed for r2B1 and r2B1 $G_{478}A$ between 1 and 80 μM BBT (*35*, *36*). When the BBT concentration was increased above 180 μM, a spectral change to a Type II spectrum occurred with both enzymes (data not shown). Two spectral binding constants for BBT were obtained for each enzyme. The binding constants determined for r2B1 and BBT were 30 μM and 0.3 mM. The high-affinity binding constant for r2B1 $G_{478}A$ and BBT was 39 μM, and the low-affinity binding constant was 1.4 mM.

Metabolite Analysis. BBT and four metabolites were identified by HPLC from ethyl acetate extracts of reconstituted r2B1. These metabolites corresponded to 1-aminoben-

Table 1: Metabolites Formed by P450 r2B1 and P450 r2B1 $G_{478}A$[a]

	ABT[b]	benzotriazole	benzaldehyde	BBT	#27
r2B1	4.9 ± 1.7	6.3 ± 3.1	5.7 ± 2.0	40 ± 28	43 ± 28
$G_{478}A$	nd[c]	nd	nd	32 ± 27	69 ± 26

[a] Incubation and analysis conditions were as described in Experimental Procedures. The values shown represent the mean standard deviation of six to seven experiments. [b] Percent metabolite formed derived from the ratio of the area of the metabolite to the area of the total metabolites in the sample. [c] nd, none detected.

zotriazole, benzotriazole, benzaldehyde, and #27 (Table 1). Previous studies using purified rat 2B1 in a reconstituted system yielded the same metabolites as seen here for the bacterially expressed protein (*22*). With the P450 r2B1 $G_{478}A$ mutant only BBT and #27 were observed. These results suggest that 2B1 became inactivated when ABT, benzotriazole, and benzaldehyde were produced. Although #27 was generated by both enzymes, it was not involved in mechanism-based inactivation since the mutant enzyme produced only #27 and was not inactivated. The apparent K_m and k_{cat} values for r2B1 $G_{478}A$ with BBT were determined with radiolabeled BBT as described in Experimental Procedures, yielding values of 0.3 mM and 12 nmol $nmol^{-1}$ min^{-1}, respectively.

Identification of #27. With the HPLC solvent conditions used in this analysis, #27 eluted off the reverse-phase C_{18} column approximately 25 min after 4-hydroxy-BBT (21 min), BBT (22.9 min), and α-methyl-BBT (23.3 min), suggesting that #27 was either more hydrophobic or larger than BBT (*22* and data not shown). Previous observations indicated that #27 was not a product of the cleavage of BBT since #27 still contained radiolabel when the reactions were carried out with BBT labeled either on the 7-benzyl carbon or on the 2/3 carbons of the aminobenzotriazole moiety (*22*). Compound #27 displayed a UV spectrum with an prominent absorption peak at 329 nm. BBT does not absorb in this region, and 4-hydroxy-BBT had a weak absorption peak at 350 nm. These observations suggested that #27 may contain a conjugated ring structure.

Natural abundance ^{13}C NMR spectra were obtained for #27 and compared with reference spectra of BBT and ABT. The BBT carbons were assigned by comparing published spectra of benzotriazole-1-acetic acid (Stadtler index no. 7056C) and benzylamine (Stadtler index no. 140C) with the spectra obtained for ABT and BBT. The spectrum of #27 was most similar to that of BBT (Table 2). The largest shifts were seen for the carbons 7 and 1 on the benzyl moiety of BBT. These observations would be consistent with a modification of carbon 7 of BBT.

The possibility that carbon 7 was oxidized to a carbonyl was tested. Samples containing benzoic acid, benzaldehyde, or benzoylhydrazine together with radiolabeled #27 obtained from the oxidation of [^{14}C]-7-BBT were acid hydrolyzed and resolved by RP-HPLC as described in Experimental Procedures. The elution times for acid-hydrolyzed benzoic acid, benzaldehyde, and benzoylhydrazine were 7.3, 9.8, and 12.3 min, respectively. In all three samples, radioactivity from #27 was associated with a peak at 9.8 min, suggesting that acid hydrolysis of #27 resulted in the formation of benzaldehyde. Similarly, samples containing #27 were acidified to a final concentration of 1 M HCl and incubated at room temperature for 2 h. HPLC analysis of these acidified

Table 2: ^{13}C NMR Resonance Peaks of ABT, BBT, and #27

	ppm		
carbon[a]	ABT	BBT	#27
7		54.17	88.70
2′	110.40	108.19	108.43
3′	118.75	116.49	116.99
4′	125.06	122.76	123.70
4		125.78	126.78
5′	128.15	125.84	126.78
2/6		126.25	127.12
3/5		127.06	127.12
1′	132.72	130.31	130.59
1		134.31	152.90
6′	144.22	141.61	142.81

[a] Carbons 1−7 correspond to the benzyl moiety carbons and 1′−6′ to the aminobenzotriazole carbons.

samples yielded benzaldehyde and residual #27. Acid hydrolysis of a carbonyl-modified BBT (*N*-benzoyl-1-aminobenzotriazole) would be expected to yield benzoic acid. In addition, FT-IR spectroscopy indicated that the spectrum of #27 did not contain a carbonyl stretch at 1640 nm. The reason a carbonyl stretch was not observed was not due to the limit of detection. Metabolite #27 gave a FT-IR spectrum with prominent stretches in the aromatic and alkyl regions. In addition, the FT-IR spectrum of benzoylhydrazine at a comparable concentration resulted in a clear carbonyl signal at 1640 nm. Together, these results suggested that #27 was not *N*-benzoyl-1-aminobenzotriazole. Oxidation to a BBT alcohol was considered unlikely since such a molecule would not be stable to the isolation procedures but would be expected to dissociate into benzoic acid and benzyl alcohol in aqueous solutions.

Electrospray mass spectrometry generated m/z^- fragments of 407 and 421 and m/z^+ fragments of 408 and 423 (Figure 4A and data not shown). FAB^+ analysis generated fragments with sizes 135, 177, 355, 373, and 445 (Figure 4B). Laser desorption mass spectrometry yielded m/z^+ fragments of 197, 287, and 422 (Figure 4C). These masses would be consistent with fragments of a rearranged oxidized BBT-like dimer after loss of four aminotriazole nitrogens from two molecules of BBT (Scheme 1). The same mass and mass fragments would also be obtained if #27 were a dimeric peroxy species. This possibility could be ruled out since mild acid treatment of #27 did not result in H_2O_2 release (data not shown).

The proton NMR spectrum of #27 showed that this compound contained at least 20 protons, a number more consistent with a BBT-like dimer (data not shown). The proton integration value may be underestimated because of a weak signal to noise ratio. None of the protons were exchangable with acid (data not shown).

Active Site Modeling. The active site model for 2B1 was used to test the effect of a glycine 478 to alanine mutation on the binding of either benzphetamine or BBT. Benzphetamine could be docked into the active site of the wild-type P450 2B1 model and was also accommodated equally well into the mutant enzyme. When the glycine at position 478 was replaced with alanine, the alanine side chain was still too far from the substrate to effect benzphetamine binding (Figure 5). This model was consistent with the experimental observation that both enzymes generated formaldehyde at the same rate. BBT could be docked in the active site of the wild-type enzyme in a number of different orientations,

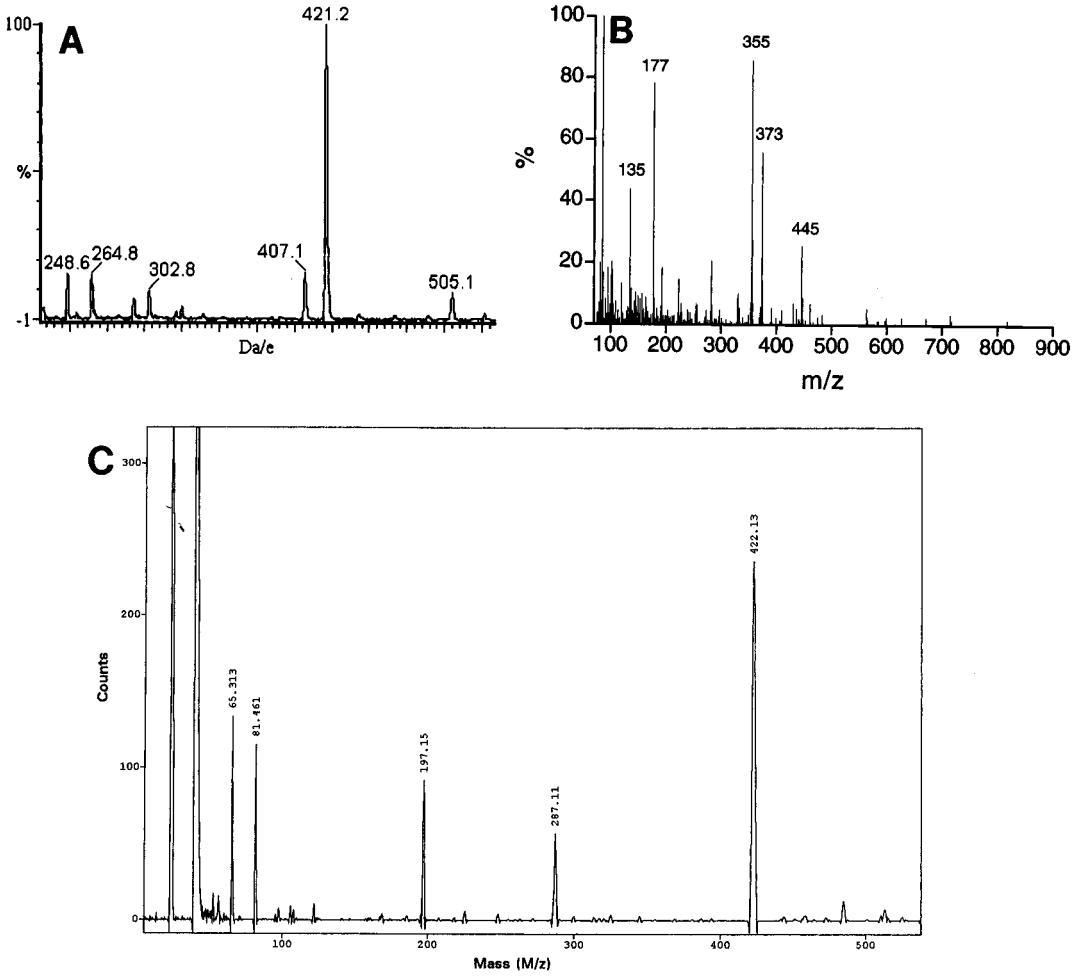

FIGURE 4: Mass spectra of #27. (A) Electrospray$^-$ mass spectrum, (B) FAB$^+$ mass spectrum, and (C) laser desorption$^+$ mass spectrum.

Scheme 1: Fragments Obtained from FAB$^+$, Laser Desorption, and Electrospray Mass Analysis

Method	Observed Mass	Expected Mass	Composition
Electrospray$^-$	421	422	422
	407	408	422 - N
FAB$^+$	445	444	422 + Na
	373	372	196 + 176
	355	354	339 + Na
	177	176	176
	135	134	134
Laser desorption$^+$	422	422	422
	287	286	196 + 90
	197	196	196

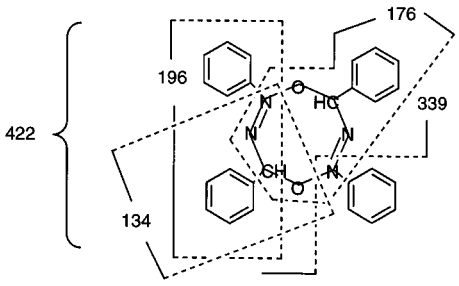

leading to oxidation at either the 1-amino nitrogen or the 7-benzyl carbon (data not shown). The modeling was again completely consistent with the experimental observation that ABT, benzotriazole, and benzaldehyde, presumably from oxidation at the 1-amino nitrogen, and #27 from the oxidation at the 7-carbon of the benzyl group were produced by the wild-type enzyme.

However, when glycine at position 478 in the model was replaced with alanine, the orientation that would allow for oxidation at the 1-amino nitrogen of the ABT moiety resulted in van der Waals overlaps between the alanine side chain and BBT (Figure 6A). Therefore, binding of BBT in this orientation in the mutant enzyme was considered unfavorable. In contrast, BBT could be easily accommodated into the active site of the $G_{478}A$ mutant model if the molecule was oriented such that oxidation at the 7 carbon of the benzyl group could occur (Figure 6B). These molecular modeling observations are consistent with our experimental results depicted in Table 1 that show that the mutant enzyme produced only #27.

Effect of ABT on the 7-EFC Activity and P450 Heme Content of P450 r2B1 and r2B1 $G_{478}A$. The 2B1 active site model predicted that the mutation at glycine 478 imposed a steric constraint on the BBT molecule such that oxidation was only possible at the 7-benzyl carbon. Since oxidation of BBT by the $G_{478}A$ mutant generated only #27 and did not inactivate the enzyme, this suggested that oxidation at the 1-amino nitrogen was required to produce the inactivating radical and the metabolites ABT, benzotriazole, and benzaldehyde. If the benzyl ring imposed the steric constraints predicted by the model, then removal of the benzyl ring should allow the molecule to orient into a position that would again lead to oxidation at the 1-amino nitrogen. The wild-type and the mutant 2B1 enzymes were incubated with the mechanism-based inactivator ABT to test if the lack of inactivation by BBT of the $G_{478}A$ mutant was due to steric

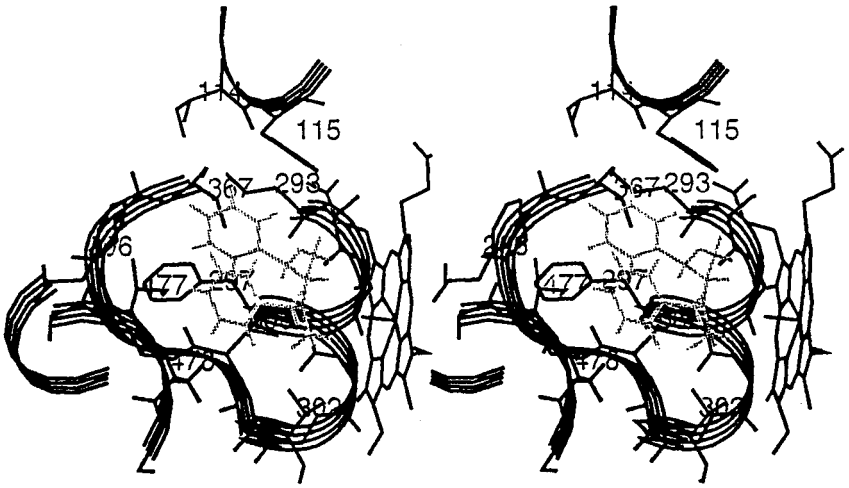

FIGURE 5: Model of benzphetamine binding in the P450 2B1 active site model. The protein backbone and ribbon are shown in black, the substrate is in gray, and the heme is in black. The side chain residues of amino acids that are within 5 Å of the substrate are numbered. Residues 114, 302, 363, 367, and 477 have been implicated in binding other substrates.

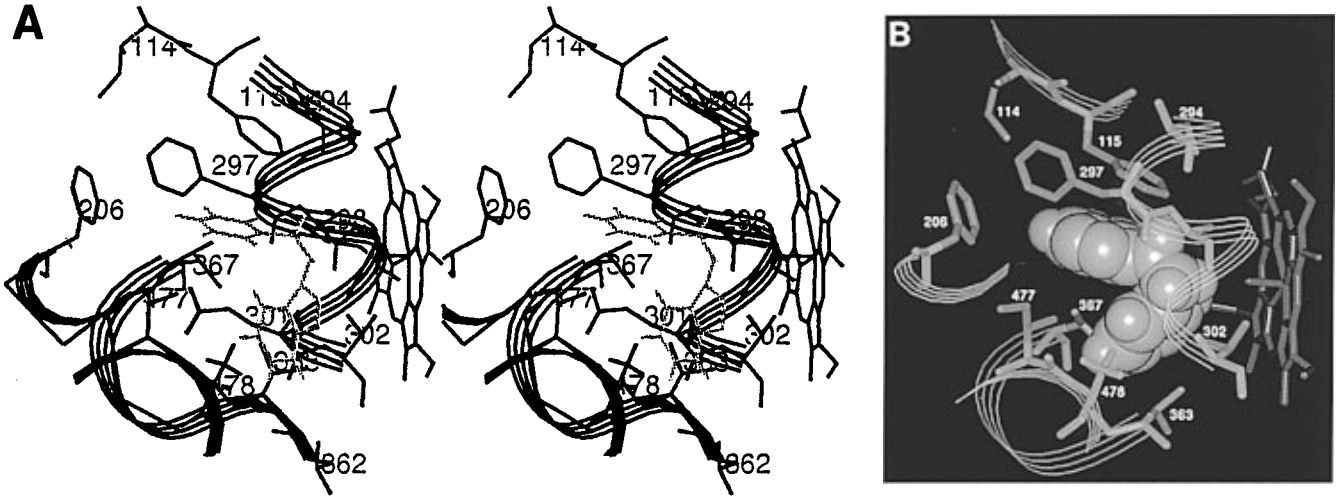

FIGURE 6: Model of BBT binding in the active site model of P450 2B1 $G_{478}A$. (A) Orientation of BBT allowing for oxidation at the 1-amino nitrogen of the aminobenzotriazole moiety. Color designations and assignments are as described in Figure 5. (B) Orientation allowing for oxidation at the 7 carbon of the benzyl moiety. The protein backbone and ribbon are shown in light blue, the substrate is in yellow, heme is in red, and alanine 478 is in green. The side chain residues of amino acids that are within 5 Å of the substrate are numbered.

Table 3: Effect of ABT on the 7-EFC *O*-Deethylation Activity of P450 r2B1 or r2B1 G478A and Cytochrome P450 Content[a]

	% activity remaining		% P450 remaining	
primary reaction	0 min	5 min	0 min	5 min
r2B1				
−ABT, −NADPH	100	96	100	99
+ABT, −NADPH	74	70		93
+ABT, +NADPH	89	26		84
$G_{478}A$				
−ABT, −NADPH	100	94	100	97
+ABT, −NADPH	97	97		97
+ABT, +NADPH	102	31		75

[a] Assay conditions were as described under Experimental Procedures. The values shown represent the avearage of two separate experiments.

hindrance of the BBT benzyl group. When r2B1 was incubated with 1 mM ABT, only 37% residual 7-EFC activity was observed after 5 min (Table 3). The same sample retained 84% of its ability to form a CO complex. Samples that had been incubated only with ABT but without NADPH had a small initial loss in activity that did not increase during the course of the assay. This initial loss at time 0 was probably due to carryover of ABT into the secondary reaction mixture. When the mutant $G_{478}A$ was incubated with ABT and NADPH for 5 min, 31% enzyme activity and 75% of the chromophore remained. These results indicate that without the BBT benzyl group the mutant was able to oxidize ABT at the 1-amino nitrogen leading to enzyme inactivation.

DISCUSSION

A number of amino acid residues (114, 206, 209, 290, 302, 363, 367, 477, 478, and 480) have been shown to play a key role in determining substrate specificity of rat P450 2B1 (*6*, *7*, *10*, *33*, *38*, *39*). In the present study the 7-pentoxyresorufin *O*-deethylation activity in microsomes from phenobarbital-induced Fischer rats was inactivated with BBT whereas the *O*-deethylation activity in Wistar−Munich microsomes was not inactivated. Although 2B1 is the major P450 enzyme induced in livers of phenobarbital treated rats, it could not be completely ruled out that the effect seen in microsomes was entirely due to 2B1. Consequently, a 2B1 $G_{478}A$ mutant that differed at only a single codon was generated and expressed in *E. coli*. The wild-type and the mutant enzyme metabolized benzphetamine at the same rate and displayed saturation with reductase to the same extent.

The rate of formaldehyde formation was comparable to values previously reported for the purified rat enzyme (*6*, *40*). In addition, both recombinant enzymes exhibited the same binding constant for the Type II spectrum induced by *n*-octylamine. The binding constants observed (1.3 μM) for the bacterially expressed purified enzymes compared well with those published for purified rat 2B1 (5 μM) (*41*). These observations with a classical 2B1 substrate and ligand suggested that the amino acid change introduced had not significantly affected the structure of the mutant enzyme.

Consistent with previous observations with purified reconstituted rat 2B1 (*22*), metabolism of BBT by r2B1 resulted in a small decrease in the absorbance of the Soret peak at 418 nm over the course of the assay with a concurrent increase at 453 nm. Presumably, the increase at 453 nm represents the formation of a metabolite intermediary complex. It has been suggested that metabolite intermediary complexes are formed by *N*-oxidation of 2′ or 3′ amine intermediates that form stable complexes with the Fe(II) of reduced cytochrome P450 (*42*, *43*). The $G_{478}A$ mutant enzyme did not form a peak at 453 nm when incubated with BBT and NADPH.

Both enzymes displayed two spectral binding constants with BBT. Several reasons could account for the two binding constants seen with each enzyme. The two binding constants may reflect two different orientations of BBT. This may be the case for P450 2B1 where ABT, benzotriazole, and benzaldehyde were formed from oxidation at the 1-amino nitrogen and #27 from oxidation at the 7-benzyl carbon. Alternatively, the P450 2B1 protein may have two distinct binding sites as has been suggested for P450 3A4 (*44*), although sigmoidal kinetics were not observed when the BBT metabolism rates by r2B1 $G_{478}A$ were analyzed. Another possibility is that the P450 2B1 active site may be able to accommodate more than one molecule of BBT. Shou et al. observed simultaneous binding of phenanthrene and 7,8-benzoflavone with P450 3A4 (*45*). Also, cytochrome P450eryF was recently crystallized with two androstenedione molecules in the active site.[3] Although the active sites of P450 3A4 and P450eryF are thought to be considerably larger than that of 2B1, 2B1 might be able to accommodate more than one smaller substrate molecule. Molecular modeling of the 2B1 enzyme predicted an upper and a lower pocket in the 2B1 active site (*33*). Whether binding of one BBT molecule introduces spatial changes in the active site to allow for a second BBT molecule to bind is not known. Studies with a number of mechanism-based inactivators have shown that the inactivated P450 2B1 can still carry out 7-EFC oxidation when alternate oxidants such as iodosobenzene or cumene hydroperoxide were used (*11*, *22*, *46*). These results suggest that the substrate binding site of 2B1 was large enough to still accommodate 7-ethoxy-4-(trifluoromethyl)-coumarin and iodosobenzene even when the active site was modified with an inactivating molecule of considerable size such as a phenanthryl acetyl group.

The binding of BBT to either r2B1 or r2B1 $G_{478}A$ also resulted in two types of difference spectra. Similar observations were made with P450 aromatase and 2-phenylpyridine, which forms a reverse Type I difference spectrum at low concentrations and a Type II spectrum at high concentrations of substrate (*47*). Spectral binding studies on wild-type 2B1 also showed a shift from a Type I to a Type II difference spectrum with increasing concentrations of miconazole.[4]

A combination of different techniques was used to derive the putative structure of #27. #27 was not an artifact of the sample workup. When the incubation mixtures were centrifuged in Centricon-30 concentrators and the supernatant was injected onto the reverse-phase column without ethyl acetate extraction, only chromatography peaks corresponding to #27 and BBT were observed.

At present it is not known where the #27 dimer was formed. Presumably dimerization does not occur in solution with two transient free radical intermediates since samples incubated with 10 mM GSH still generate #27 (*22*). Alternatively, dimerization could occur in the 2B1 enzyme if two BBT molecules remain in or near the active site long enough to be oxidized and to dimerize. However, the mechanism whereby this might occur is not clear.

Although rabbit P450 2B4 and 2B5 exhibit different substrate specificities, they differ by only 12 amino acids (*48*). Residues 114, 294, 363, and 367 were found to be important in the regio- and stereoselectivity of androstenedione hydroxylation (*49*). The apparent K_I for BBT with 2B4 or 2B5 in hepatic microsomes was similar (1.9 and 2.4 μM), and the observed rate constants were 0.29 and 0.18 min^{-1}, respectively (*50*). These results suggested that BBT did not distinguish between 2B4 and 2B5. P450 2B2 differs for P450 2B1 by 13 amino acids including the glycine 478 to alanine change (*25*). Interestingly, the 7-EFC activity of P450 2B2 like that of the $G_{478}A$ mutant was not inactivated by BBT (data not shown). Together, these observations emphasize again the significance of glycine 478 in P450 2B1 in the metabolism of BBT to inactivating metabolites. Selective inactivators are important tools in elucidating the catalytic mechanism of closely related isoforms and the role individual P450s play in the metabolism of xenobiotics and endobiotics to cytotoxic or carcinogenic metabolites. As demonstrated in this study the P450 2B1 active site model was completely consistent with the BBT metabolism studies. Therefore, the P450 2B1 model can serve as a valuable tool in the design of isoform-specific inhibitors or inactivators.

ACKNOWLEDGMENT

The authors thank Tracie Shand for electrospray mass spectromerty of BBT and #27 and James Epperson for the laser desorption analysis of #27.

REFERENCES

1. Nelson, D. R., Koymans, L., Kamataki, T., Stegeman, J. J., Feyereisen, R., Waxman, D. J., Waterman, M. R., Gotoh, O., Coon, M. J., Estabrook, R. W., Gunsalus, I. C., and Nebert, D. W. (1996) *Pharmacogenetics 6*, 1−42.
2. Porter, T. D., and Coon, M. J. (1991) *J. Biol. Chem. 266*, 13469−13472.
3. Gonzalez, F. J. (1989) *Pharmacol. Rev. 40*, 243−288.
4. Guengerich, F. P. (1993) *Drug Metab. Dispos. 21*, 1−6.
5. Waxman, D. J. (1988) *Biochem. Pharmacol. 37*, 71−84.
6. Kedzie, K. M., Balfour, C. A., Escobar, G. Y., Grimm, S. W., He, Y.-A., Pepperl, D. J., Regan, J. W., Stevens, J. C., and Halpert, J. R. (1991) *J. Biol. Chem. 266*, 22515−22521.
7. Aoyama, T., Korzekwa, K., Nagata, K., Adesnik, M., Reiss, A., Lapenson, D. D., Gillette, J., Gelboin, H. V., Waxman, D. J., and Gonzalez, F. J. (1989) *J. Biol. Chem. 264*, 21327−21333.

[3] Cupp-Vickery and Poulos, personal communication.
[4] Hanna, unpublished results.

8. Matsunaga, E., Zeugin, T., Zanger, U. M., Aooyama, T., Meyer, U. A., and Gonzalez, F. J. (1990) *J. Biol. Chem. 265*, 17197−17201.
9. Traber, P. G., Wang, W., McDonnell, M., and Gumucio, J. J. (1990) *Mol. Pharmacol. 37*, 810−819.
10. He, Y.-A., Balfour, C. A., Kedzie, K. M., and Halpert, J. R. (1992) *Biochemistry 31*, 9220−9226.
11. Roberts, E. S., Hopkins, N. E., Alworth, W. L., and Hollenberg, P. F. (1993) *Chem. Res. Toxicol. 6*, 470−479.
12. Roberts, E. S., Hopkins, N. E., Zaluzec, E. J., Gage, D. A., Alworth, W. L., and Hollenberg, P. F. (1995) *Arch. Biochem. Biophys. 323*, 295−302.
13. He, K., Falick, A. M., Chen, B., Nilsson, F., and Correia, M. A. (1996) *Chem. Res. Toxicol. 9*, 614−622.
14. Straub, P., Loyd, M., Johnson, E. F., and Kemper, B. (1994) *Biochemistry 33*, 8029−8034.
15. Johnson, E. F., Kronbach, T., and Hsu, M. H. (1992) *FASEB J. 6*, 700−705.
16. Negishi, M., Iwasaki, M., Juvonen, R. O., Sueyoshi, T., Darden, T. A., and Pedersen, L. G. (1996) *Mutat. Res. 350*, 43−50.
17. Rampersaud, A., and Walz, F. G., Jr. (1987) *Biochem. Genet. 25*, 527−534.
18. Szklarz, G. D., Ornstein R. L., & Halpert, J. R. (1994) *J. Biomol. Struct. Dyn. 12*, 61−77.
19. Woodcroft, K. J., Szczepan, E. W., Knickle, L., C., and Bend, J. R. (1990) *Drug Metab. Dispos. 18*, 1031−1037.
20. Woodcroft, K. J., and Bend, J. R. (1990) *Can. J. Physiol. Pharmacol. 68*, 1278−1285.
21. Woodcroft, K. J., Webb, C. D., Yao, M. Weedon, A. C., and Bend, J. R. (1997) *Chem. Res. Toxicol. 10*, 589−599.
22. Kent, U. M., Bend, J. R., Chamberlin, B. A., Gage, D. A., and Hollenberg, P. F. (1997) *Chem. Res. Toxicol.* 10, 600−608.
23. Mathews, J. M., and Bend, J. R. (1986) *Mol. Pharmacol. 30*, 25−32.
24. Barnes, H. J., Arlotto, M. P., and Waterman, M. R. (1991) *Proc. Natl. Acad. Sci. U.S.A. 88*, 5597−5601.
25. Guengerich, F. P., Martin, M. V., Guo, Z., and Chun, Y.-J. (1996) *Methods Enzymol. 272*, 35−44.
26. Hanahan, D. (1983) *J. Mol. Biol. 166*, 557−580.
27. Shen, A. L., Porter, T. D., Wilson, T. E., and Kasper, C. B. (1989) *J. Biol. Chem. 264*, 7584−7589.
28. Saito T., and Strobel, H. W. (1981) *J. Biol. Chem. 256*, 984−988.
29. Burke, M. D., Thompson, S., Elcombe, C. R., Halpert, J. R., Haaparanta, T., and Mayer, R. T. (1985) *Biochem. Pharmacol. 34*, 3337−3345.
30. Buters, J. T. M., Schiller, C. D., and Chou, R. C. (1993) *Biochem. Pharmacol. 46*, 1577−1584.
31. Nash, T. (1953) *Biochem. J. 55*, 416−421.
32. Omura, T., and Sato, R. (1964) *J. Biol. Chem. 239*, 2370−2378.
33. Szklarz, G. D., He, Y.-A., and Halpert, J. R. (1995) *Biochemistry 34*, 14312−14322.
34. He, K., He, Y. A., Szklarz, G. D., Halpert, J. R., and Correia, M. A. (1996) *J. Biol. Chem. 271*, 25864−25872.
35. Szklarz, G. D., and Halpert, J. R. (1997) *J. Comput.-Aided Mol. Des. 11*, 265−272.
36. Schenkman, J. B., Remmer, H., and Estabrook, R. W. (1967) *Mol. Pharmacol. 3*, 113−123.
37. Schenkman, J. B., Sligar, S. G., and Cinti, D. L. (1982) in *International encyclopedia of pharmacology and therapeutics: Hepatic cytochrome P-450 monooxygenase system* (Schenkmann, J. B., and Kupfer, D., Eds.) pp 587−615, Pergamon Press, Oxford, NY.
38. Halpert, J. R., and He, Y.-A. (1993) *J. Biol. Chem. 268*, 4453−4457.
39. Luo, Y., He, Y.-A., and Halpert, J. R. (1994) *Arch. Biochem. Biophys. 309*, 52−57.
40. Ryan, D. E., Thomas, P. E., and Levin, W. (1982) *Arch. Biochem. Biophys. 216*, 272−288.
41. Wilson, N. M., Christou, M., Turner, C. R., Wrighton, S. A., and Jefcoate, C. R. (1984) *Carcinogenesis 5*, 1475−1483.
42. Werringloer, J., and Estabrook, R. W. (1973) *Life Sci. 13*, 1319−1330.
43. Bast, A., Savenije-Chapel, E. M., and Noordhoek, J. (1984) *J. Pharm. Sci. 73*, 953−956.
44. Ueng, Y.-F., Kuwabara, T., Chun, Y.-J., and Guengerich, F. P. (1997) *Biochemistry 36*, 370−381.
45. Shou, M., Grogan, J., Mancewicz, J. A., Krausz, K. W., Gonzalez, F. J., Gelboin, H. V., and Korzekwa, K. R. (1994) *Biochemistry 33*, 6450−6455.
46. Roberts, E. S., Ballou, D. P., Hopkins, N. E., Alworth, W. L., and Hollenberg, P. F. (1995) *Arch. Biochem. Biophys. 323*, 303−312.
47. Vaz, A. D. N., Coon, M. J., Peegel, H., and Menon, K. M. J. (1991) *Drug Metab. Dispos. 20*, 108−112.
48. Kedzie, K. M., Philpot, R. M., and Halpert, J. R. (1991) *Arch. Biochem. Biophys. 291*, 176−186.
49. Szklarz, G. D., He, Y. Q., Kedzie, K. M., Halpert, J. R., and Burnett, V. L. (1996) *Arch. Biochem. Biophys. 377*, 308−318.
50. Grimm, S. W., Bend, J. R., and Halpert, J. R. (1995) *Drug Metab. Dispos. 23*, 577−583.

BI971064Y